

greatest for the U-Net trained on the 1st echo (-0.58) followed by the U-Net trained on all echoes (-0.47) and the manual segmentations (-0.36, Table 2). Longitudinally, KLG 0 knees with CL JSN tended to show a greater increase in deep layer T2 than KLG 0 knees with CL KLG 0, but most differences did not reach statistical significance (Table 3). The greatest Cohen's D was observed for the entire FTJ with the U-Net trained on all echoes (-0.59) followed by manual segmentations (-0.50) and the U-Net trained on the 1st echo only (-0.47, Table 3). In the superficial layer, all segmentation methods (manual, all-echoes U-Net, 1st-echo U-Net) showed similar, small changes for both KLG 0 knees with CL JSN and with CL KLG 0 (Table 3). **Conclusions:** Although the U-Nets tended towards an over-segmentation, the U-Nets applied to MESE MRIs showed high agreement with manual femorotibial cartilage segmentations and only small systematic differences. Training the U-Net on all available echoes had no obvious advantage over training the U-Net on the 1st echo only. When applied to KLG 0 knees with CL JSN vs. CL KLG 0, the U-Net segmentation was able to reproduce the differences previously observed for manual segmentations with an effect size that was at least comparable with that observed for manual segmentations. The U-Net-based cartilage segmentation from MESE MRIs may therefore be a promising tool for future studies focusing on cartilage T2 analyses.

#### 100 DEVELOPMENT OF THE PROTO-KNEE TOOL USING MACHINE LEARNING ALGORITHMS TO PREDICT CLINICAL OUTCOMES AFTER TOTAL KNEE ARTHROPLASTY

Y. Zhou, C. Schilling, M. Dowsey, P. Choong. *Univ. of Melbourne, Melbourne, Australia*

**Purpose:** Recent literature reports that 1 in 5 patients feel unsatisfied after total knee arthroplasty (TKA). This is associated with significant burdens to the healthcare system. Improving patient selection can reduce the proportion of patients who experience non-beneficial surgery. Prognostic tools may aid in the patient selection process. The purpose of this study is to use machine learning algorithms to develop a prognostic tool to predict outcomes in TKA. Unlike many other prognostic tools, the PROTO-KNEE tool aims to be used independently by the patient without clinician input.

**Methods:** The St. Vincent's Melbourne Arthroplasty Outcomes (SMART) Registry prospectively collected all TKA procedures performed at their institute from April 2000 onwards. Using the SMART Registry, patient variables and outcomes were evaluated for predictive model building. Pre-operative variables considered for prediction included demographics, co-morbidities, socioeconomic status, body-mass index (BMI), and responses to the Veterans-Rand-12 (VR-12) survey. Predicted outcome of interest was change in utility score at 12 months post-surgery, guided by previously validated minimal clinically important difference (MCID) values. Recursive feature elimination was used to select features that optimised algorithm performance. Three machine learning algorithms and 2 regression models were developed with a training sample of patients using 10-fold cross-validation. These models were subsequently applied to a testing sample of patients and assessed by discrimination, calibration, and decision curve analysis.

**Results:** 7509 patients with primary unilateral TKA with a minimum of 12 months follow up were included in the model development dataset. Change in utility score by an MCID of 0.09 was used to determine the improvement / no improvement threshold. Random forest algorithm achieved the best performance with the testing sample (2000 trees, accuracy: 0.738, c-statistic: 0.825, Brier score: 0.161). The most important factors for predicting post-operative improvement were age, gender, pre-operative BMI and VR-12 survey responses.

**Conclusions:** This study developed a machine learning algorithm to predict improvement after TKA. Our model demonstrated a high discriminative capacity for patient-specific factors and identified key predictors that may influence post-operative outcomes. Further studies are required to externally validate this tool in non-Australian populations and evaluate the tool in the setting of a prospective clinical trial.

#### 101 IPRIFLAVONE-LOADED POLY(D,L-LACTIDE-CO-GLYCOLIDE) ACID NANOPARTICLES FOR THE TREATMENT OF OSTEOARTHRITIS

C. Remírez de Ganuza<sup>1</sup>, M. Paesa<sup>1</sup>, F. García-Álvarez<sup>1</sup>, M. Rodríguez-Yoldi<sup>1</sup>, S. Irusta<sup>1</sup>, M. Arruebo<sup>1</sup>, G. Mendoza<sup>2</sup>. <sup>1</sup>Univ. de Zaragoza, Zaragoza, Spain; <sup>2</sup>Aragon Hlth.Res. Inst., Zaragoza, Spain

**Purpose:** Osteoarthritis (OA) is a degenerative disease that affects the entire joint and is characterized by the destruction of cartilage, alterations in the structure of the subchondral bone and chronic inflammation of the synovial membrane, which entails pain and joint stiffness, and therefore the deterioration of the patient's quality of life. OA has no cure, and current treatments are palliative, aimed at relieving symptoms, mainly through drugs, and ultimately by surgery. Therefore, the development of novel and effective treatments capable of reducing symptoms and stopping the progression of the disease is necessary. Ipriflavone (IP) is capable of inhibiting cartilage degeneration and exhibits great anti-inflammatory potential. Furthermore, nanotechnology has arisen in the last decades as a promising field of study in drug delivery, improving drug targeting and localized drug delivery by providing a sustained or controlled delivery to prolong the therapeutic effect. In this context, IP encapsulation in nanosystems of poly (lactico-glycolic acid) (PLGA) would allow a controlled release compared to the local administration of the free synthetic isoflavone. The aim of this study was to synthesize and characterize PLGA nanoparticles (NPs) containing IP and evaluate their cytotoxicity and capacity to attenuate cartilage degeneration and inflammation on human osteoarthritic chondrocytes. The ultimate goal is to show a demonstrated benefit of the encapsulation of the drug compared to the administration of the equivalent dose of the free compound.

**Methods:** Patients' samples were obtained from total knee replacement surgeries performed in the Hospital Clínico Universitario Lozano Blesa (Zaragoza, Spain). Patients' consent and ethics committee approval (PI20/429) were granted by the Aragon Government. Primary human articular chondrocytes were obtained from cartilage slices cut from macroscopically osteoarthritic cartilage of replaced knees. Type II collagenase was used to digest the slices and obtain the cells, which were seeded at a cell density of 10<sup>5</sup> in flasks of 25 cm<sup>2</sup>. When chondrocytes were confluent, cells were passaged and the subsequent experiments were performed in early passages (passages 1 and 2). First, cell viability and apoptosis were evaluated after treatment with IP (5 and 10 μM) for 24h. Blue Cell Viability Assay was used to test cell viability, the reagent was added to the cells (10%) and after incubation, fluorescence was measured. To analyse cell apoptosis, cells were centrifuged and the pellet was resuspended in Annexin-binding buffer, stained with Annexin V-FITC and analyzed by flow cytometry in a Gallios equipment. On the other hand, PLGA NPs were synthesized using the simple emulsification-solvent evaporation method, loading the inner core of the emulsion with IP (10 μM). To assess the morphology and size of the particles, they were analysed by scanning electron microscopy (SEM) and transmission electron microscopy (TEM). NP size and size distribution were determined by Dynamic Light Scattering (DLS). The drug content in NPs was determined directly by measuring the encapsulated IP amount in PLGA NPs after dissolution using UV-Visible at 298 nm. Lastly, the cytotoxicity of free IP and the PLGA nanosystems in primary human chondrocytes were evaluated by the Blue Cell Viability Assay, after 24h of incubation with different concentrations (0,1 -2 mg/ml) of PLGA NPs alone or loaded with IP and with the equivalent doses of free drug.

**Results:** The results obtained showed the cytocompatibility of IP at both concentrations tested. Cell viability (Fig 1A) showed percentages higher than 70% in all cases, fulfilling the recommendations of the ISO 10993-5. Furthermore, apoptosis results display that the treatment with IP does not increase cell death (Fig 1B). Based on this, 10 μM was the concentration of IP chosen to be encapsulated. The encapsulating polymer of choice was the FDA approved in many medical devices PLGA using single emulsion solvent evaporation to take advantage of the hydrophobic nature of IP assuring high drug loadings. IP encapsulation does not affect NPs morphology, as shown by SEM and TEM images (Fig 1C, E). The particle size distribution histogram (Fig 1D) obtained by analysing different SEM images shows a narrow particle size distribution, resulting in a mean diameter value of 111,9 ± 15 nm. TEM images of

negatively stained PLGA-IP NPs also revealed the lack of non-encapsulated IP crystals surrounding the PLGA spherical nanoparticles (Fig 1E). As colloidal water-based suspensions were used, size distribution was also analysed by DLS, the mean particle size obtained was  $170.7 \pm 1.9$  nm, with the polydispersity index smaller than 0.1, corroborating the monodispersity of the NPs, thus, the encapsulation of IP does not cause particle agglomeration or irreversible aggregation. The efficacy of encapsulation was also evaluated, with 6,72wt.% of IP loaded into the NPs. Finally, PLGA NPs cytotoxicity was analysed, cell viability on human primary chondrocytes was not affected by the use of PLGA nanoparticles (empty or loaded) at any of the concentrations tested (Fig 1F).

**Conclusions:** Our studies demonstrate the ability of Ipriflavone to be encapsulated in polymeric nanoparticles, as it did not show detrimental effects in primary osteoarthritic chondrocytes and is successfully encapsulated in PLGA. This would allow a controlled drug release, thus prolonging the therapeutic effect. With this scenario, it seems interesting to analyse the anti-inflammatory capacity of the IP loaded nanoparticles in chondrocytes in order to evaluate their potential use in OA long term treatment using a single administration of the encapsulated drug.

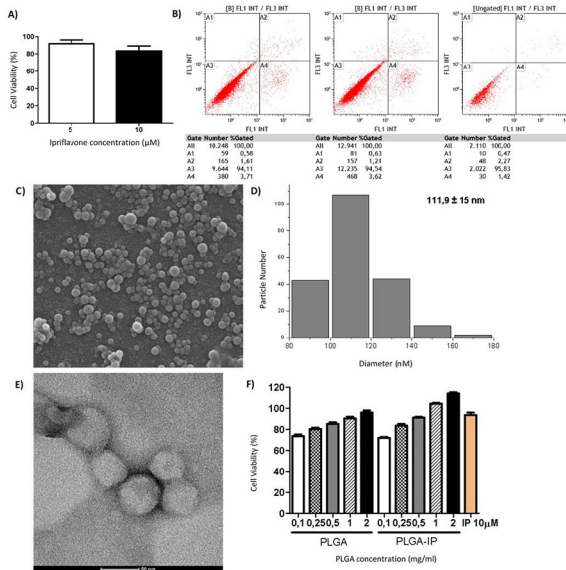


**Figure 1.** Effect of treatment of chondrocytes with different concentrations of Ipriflavone for 24 h and characterization of cytocompatibility of IP loaded NPs. A) Viability analysis by the Blue Cell Viability Assay kit. The results are expressed as a percentage of viability, taking as 100% viability, the viability of control cells not treated with IP. B) Analysis of apoptosis by flow cytometry, from left to right: control without IP, IP 5 μM, and IP 10 μM. A1: necrosis, A2: late apoptosis, A3: viable cells, A4: early apoptosis. C) SEM images of PLGA-IP particles. D) Particle size distribution histogram obtained from the measurement of 250 NPs from SEM images. E) TEM images of the PLGA-IP particles. F) Cytotoxicity of PLGA and PLGA-IP NPs in chondrocytes evaluated by the Blue Cell Viability Assay kit. Results are expressed as a percentage of viability, taking as 100% viability, the viability of control cells not treated with IP.

**102 UNSUPERVISED CLUSTERING OF KNEE OSTEOARTHRITIS HISTOLOGIC AND SONOGRAPHIC FEATURES**

**B.Y. Mehta<sup>1</sup>, M. Konnaris<sup>1</sup>, R. Bell<sup>1</sup>, T. Pannellini<sup>2</sup>, E. DiCarlo<sup>1</sup>, D. Jannat-Khah<sup>1</sup>, J. Gibbons<sup>1</sup>, O. Nwawka<sup>1</sup>, S.C. Lee<sup>1</sup>, P.K. Sculco<sup>1</sup>, M.L. Parks<sup>1</sup>, M. Fontana<sup>1</sup>, M.P. Figgie<sup>1</sup>, L.T. Donlin<sup>1</sup>, D.E. Orange<sup>3</sup>, T.P. Sculco<sup>1</sup>, W.H. Robinson<sup>4</sup>, S.M. Goodman<sup>1</sup>, M. Otero<sup>1</sup>, F. Wang<sup>2</sup>.**  
<sup>1</sup>Hosp. for Special Surgery, New York, NY; <sup>2</sup>Weill Cornell Med., New York, NY; <sup>3</sup>Rockefeller Univ., New York, NY; <sup>4</sup>Stanford Univ., Palo Alto, CA

**Purpose:** The heterogenous nature of Osteoarthritis (OA) has posed challenges to the development of disease modifying therapies, likely due to different pathogenic mechanisms underlying distinct subtypes of OA. Efforts to subtype the disease have been limited, and integrative approaches are lacking. Here, we applied unsupervised clustering analysis of histology and ultrasound data to identify clinically-relevant knee OA subtypes in patients undergoing total knee arthroplasty (TKA).

**Methods:** We prospectively enrolled 160 patients (age 45–75) with end-stage knee OA scheduled for TKA with IRB approval and patient consent. We collected clinical data, patient-reported data and ultrasounds (43 features, recorded using B-Mode and doppler and evaluated by two radiologists) preoperatively. A total of 21 histologic features were scored by two trained pathologists on hematoxylin and eosin (H&E)-stained synovial biopsies. Histology and ultrasound features with  $\geq 5\%$  of variance (n=17) from 157 subjects (with  $\leq 65\%$  missing data) were used for analyses. Min-max scaling was applied, and unsupervised clustering using Euclidean distance and agglomerative hierarchical clustering was conducted. Wilcoxon Rank Sum tests (continuous variables) and Chi squared tests (categorical variables) were performed for statistical comparisons between clusters.

**Results:** Hierarchical clustering of 12 synovial histology features and 5 ultrasound features identified 5 OA subtypes (Figure 1a-b), defined by the differences in features between subjects and named accordingly: 1) *High Inflammatory Subtype* (N=12) with high levels of inflammatory cell infiltrates including plasma cells and lymphocytes, 2) *Heterogeneous Subtype* (N=84) with little to no findings of inflammation or differences in ultrasound features, 3) *Minimal Pathology Subtype* (N=28) with presence of Baker's cysts on ultrasound and low levels of synovial inflammation histologic features, 4) *Detritic and Synovial Giant Cell Infiltration Subtype* (N=21), and 5) *Moderate Inflammatory Subtype* (N=12) with moderate levels of the same synovial features. Both the *high* and *moderate inflammatory* subtypes were associated with high BMI (p=0.048), African American (AA) race (p=0.015), increased levels of ESR (p=0.043) and HS-CRP (p=0.023). The high inflammatory subtype was associated with patient-reported major trauma to the affected joint (p=0.025) (Table 1).

**Conclusions:** Clustering analysis of synovial histology and ultrasound scoring features identified 5 OA patient subtypes. Two subtypes were associated with AA race, increased BMI, and synovial inflammation, which suggests that demographical factors may play a role in the mechanisms underlying knee OA and warrants further investigation. Our findings suggest that the clinical features and patient-reported outcomes represent predictive variables with the potential to be built into algorithms that could be used in the future to guide targeted personalized treatment of these OA subtypes.

**Figure 1: Knee OA subtypes identified by hierarchical clustering.** (A) Euclidean Hierarchical clustering revealed 5 knee OA clusters. The number of patients included in each cluster is indicated. (B) 2-D UMAP spatial representation of individual subjects by cluster.

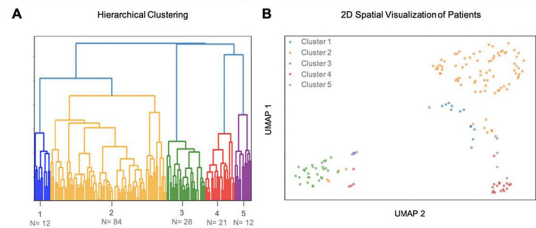


**Table 1: Patient subtypes and demographics.** Distribution of baseline demographics, clinical features, and blood biomarkers of systemic inflammation collected at the time of enrollment. Data is represented as mean ± SD. Significance is indicated in bold as P<0.05.

	All (N=157)	Cluster 1 (N=12)	Cluster 2 (N=84)	Cluster 3 (N=28)	Cluster 4 (N=21)	Cluster 5 (N=12)	P value
<b>Baseline Demographics</b>							
Age	64.9 ± 6.8	63.4 ± 8.6	65.4 ± 6.2	65.5 ± 7.3	62.8 ± 7.2	65.3 ± 7.0	0.578
Sex (Females)	61	4	36	10	8	3	0.772
BMI (kg/m <sup>2</sup> )	31.7 ± 6.7	35.4 ± 7.3	31.5 ± 6.5	30.7 ± 5.3	29.7 ± 7.0	35.3 ± 8.3	<b>0.048</b>
Race							<b>0.015</b>
African American/Black	10.2%	33.3%	2.4%	14.3%	14.3%	25.0%	
Asian	5.1%	8.3%	2.4%	0.0%	14.3%	16.7%	
Alaskan/American Indian	0.6%	0.0%	1.2%	0.0%	0.0%	0.0%	
Caucasian/White	81.5%	58.3%	91.7%	85.7%	66.7%	50.0%	
Native Hawaiian or Pacific Islander	0.6%	0.0%	0.0%	0.0%	4.8%	0.0%	
Other	1.9%	0.0%	2.4%	0.0%	0.0%	8.3%	
<b>Clinical features</b>							
Kellgren-Lawrence Score (Grade 0-4)	3.2 ± 0.8	3.7 ± 0.5	3.2 ± 0.8	3.2 ± 0.7	3.3 ± 0.8	3.1 ± 1.2	0.259
Sum of Comorbidities (0-12)	3.4 ± 2.2	3.4 ± 2.2	3.5 ± 2.2	3.5 ± 2.3	2.5 ± 1.6	4.1 ± 3.0	0.354
Cigarette Pack Years	3.8 ± 7.5	3.8 ± 6.2	3.9 ± 7.5	7.0 ± 10.6	1.1 ± 2.4	0.4 ± 1.0	0.087
Alcohol use (0-4)	1.2 ± 1.3	0.6 ± 1.0	1.5 ± 1.3	1.2 ± 1.4	1.3 ± 1.2	0.5 ± 0.7	0.137
Morning Knee Stiffness Presence	79.0%	67.0%	80.0%	86.0%	76.0%	75.0%	0.730
Major Trauma to Affected Knee	12%	8%	6%	22%	10%	33%	<b>0.025</b>
<b>Blood Biomarkers</b>							
Binarized ESR (mm/hr) (0/1)	30.0%	45.0%	21.0%	46.0%	25.0%	50.0%	<b>0.043</b>
Ordinal HS-CRP (mg/dL) (0.0 - 1.0 mg/dL) (0-5)	1.7 ± 1.7	2.6 ± 1.9	1.4 ± 1.5	2.2 ± 1.8	1.7 ± 1.7	2.3 ± 2.3	<b>0.023</b>